

Center for Advanced Materials

CAM

RECEIVED
LAWRENCE
BERKELEY LABORATORY

NOV 20 1987

LIBRARY AND
DOCUMENTS SECTION

Submitted to Zeolites

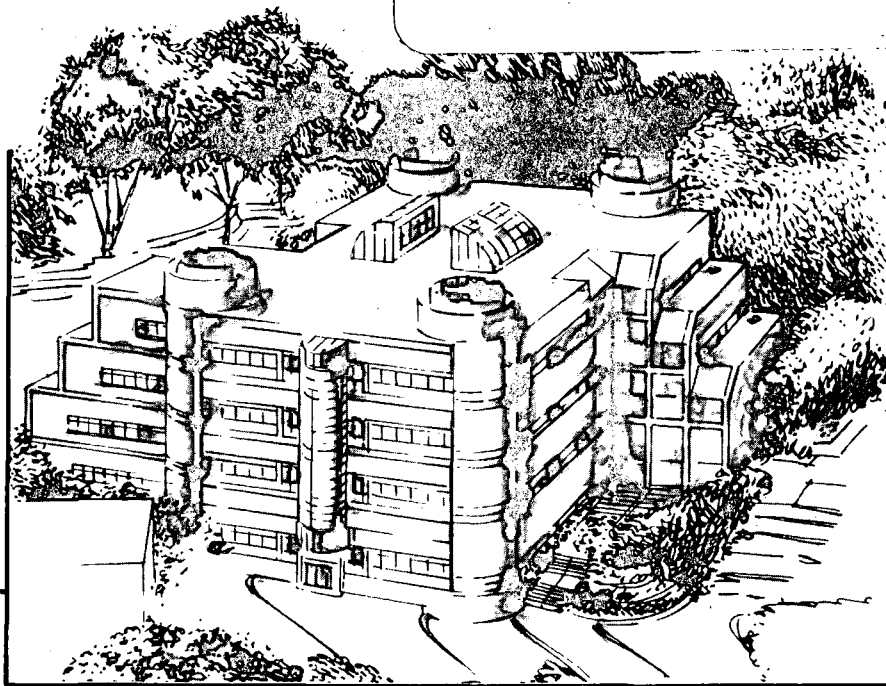
Vitrification of Zeolite Y in the TEM

R. Csencsits and R. Gronsky

September 1987

TWO-WEEK LOAN COPY

*This is a Library Circulating Copy
which may be borrowed for two weeks.*



Materials and Chemical Sciences Division

Lawrence Berkeley Laboratory • University of California

ONE CYCLOTRON ROAD, BERKELEY, CA 94720 • (415) 486-4755

LBL-22549 Rev. ^{c-2}

DISCLAIMER

This document was prepared as an account of work sponsored by the United States Government. While this document is believed to contain correct information, neither the United States Government nor any agency thereof, nor the Regents of the University of California, nor any of their employees, makes any warranty, express or implied, or assumes any legal responsibility for the accuracy, completeness, or usefulness of any information, apparatus, product, or process disclosed, or represents that its use would not infringe privately owned rights. Reference herein to any specific commercial product, process, or service by its trade name, trademark, manufacturer, or otherwise, does not necessarily constitute or imply its endorsement, recommendation, or favoring by the United States Government or any agency thereof, or the Regents of the University of California. The views and opinions of authors expressed herein do not necessarily state or reflect those of the United States Government or any agency thereof or the Regents of the University of California.

Vitrification of Zeolite Y in the TEM

R. Csencsits and R. Gronsky

Center for Advanced Materials
National Center for Electron Microscopy
Lawrence Berkeley Laboratory
University of California
Berkeley, CA 94720

ABSTRACT

The metamict transformation of Y zeolite in the transmission electron microscope (TEM) has been studied in the range of accelerating voltages 80-200 kV. This study concentrates on the effects of accelerating voltage and Si/Al-ratio. The results show that the damage is due to radiolysis and that increasing the accelerating voltage and Si/Al-ratio prolongs the observation lifetime of the zeolite. A mechanism for the metamict transformation involving the cation is proposed. This mechanism is used to suggest ways of reducing the damage rate.

INTRODUCTION

The damage of zeolites (and other silicates) upon examination in the transmission electron microscope (TEM) has been well documented.¹⁻⁶ Zeolites become amorphous during electron beam irradiation. This is known in the geological community as metamictization. Observations show that the damage rate of zeolites depends on the Si/Al-ratio, on the size of the cations,² and on the extent of hydration.¹ The goal of this work is to study the effects of varying the accelerating voltage and the Si/Al-ratio on the damage of Y zeolite in the TEM and to propose a model for the damage mechanism.

The types of damage possible in the transmission electron microscope (TEM) can be classified under two general headings: knock-on and radiolytic. "Knock-on" damage involves the interaction of the incident electron with the nucleus of an atom in the specimen. An atom is "knocked" from its site, thereby changing the structure. Radiolytic damage involves the transfer of energy from the incident electron to the valence electrons in the specimen. The increase in energy of the specimen electrons results in bond breakage and consequently the possible alteration of the structure.

Knock-on damage

The cross-section for direct interaction of the probing electron and the nuclear core of an atom in the specimen is called the knock-on cross-section. For relativistic electrons this cross-section is given by^{7,8}

$$\sigma_n = \left\{ \frac{4\pi a_0^2 U_R^2}{(mc^2)^2} \right\} \left\{ \frac{Z^2(1-\beta^2)}{\beta^4} \right\} \left\{ \left(\Omega_r \right) + 2\pi\alpha\beta \left(\Omega_r \right)^{1/2} - (\beta^2 + \pi\alpha\beta) \ln \left(\Omega_r \right) - 1 - 2\pi\alpha\beta \right\} \quad (1)$$

where:

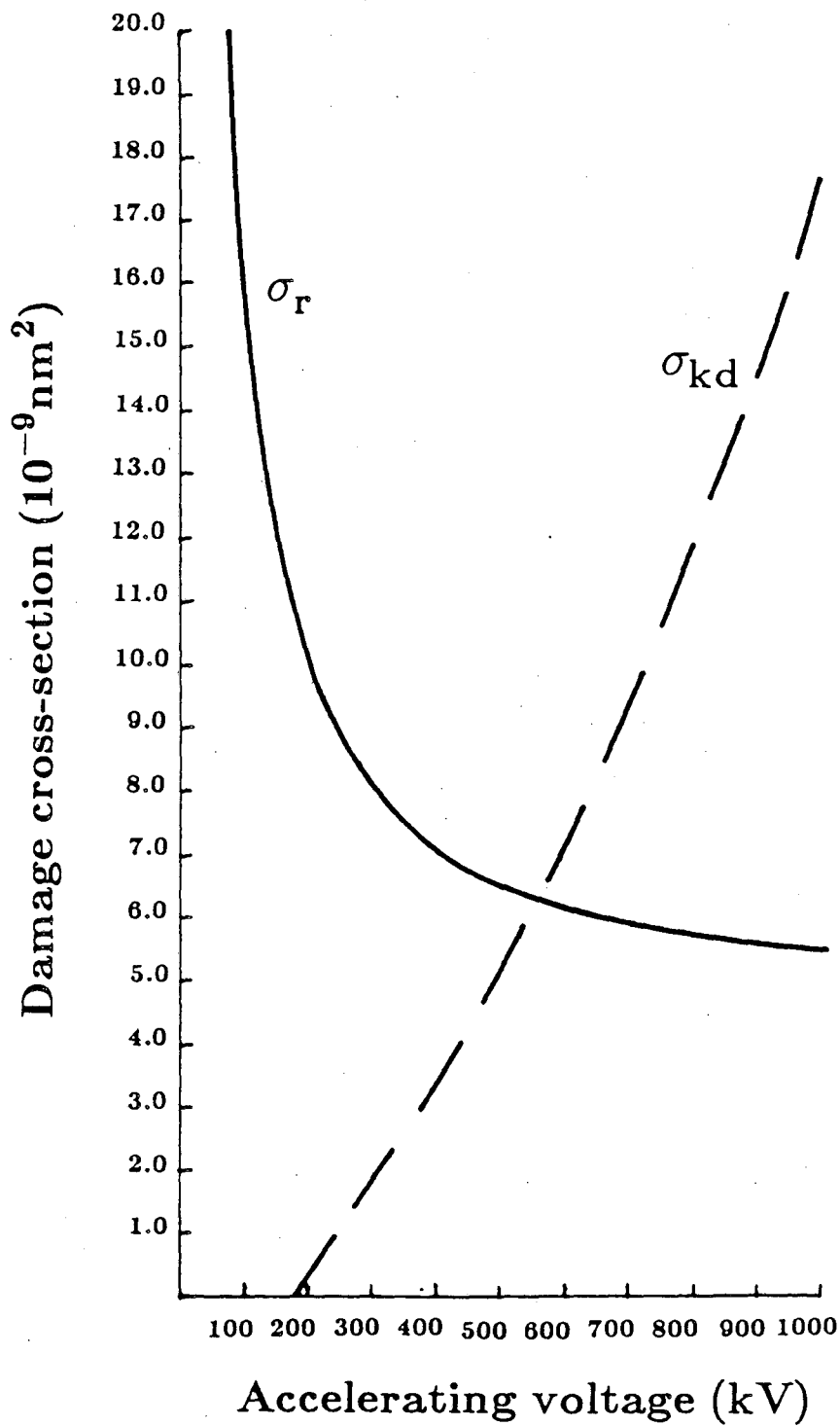
$$\Omega_r = \frac{T_{\max}}{T_{th}} \quad T_{\max} = \frac{2 U_p (U_p + 2mc^2)}{Mc^2}$$

$$\beta = \left\{ 1 - \frac{1}{\left(\frac{U_p}{mc^2} + 1 \right)^2} \right\}^{1/2}$$

U_p is the incident beam kinetic energy (keV), and mc^2 is the rest energy of the electron (511 keV). Mc^2 is the rest energy of the nucleus, α is $Z/137$, Z is the atomic number, U_R is the Rydberg constant (0.0136 keV), and a_0 is the Bohr radius (0.053 nm). The maximum energy that an incident electron can transfer to a nucleus is T_{\max} . The minimum energy necessary to move an atom off its lattice site into some metastable position is T_{th} , which depends directly on the atomic number.

All materials undergo direct displacement of atoms above their specific threshold energy. For most metals the threshold energy, T_{th} , is 20-30 eV and $\sigma_n=0$ for accelerating voltages under 300 kV. However for lighter elements such as Al (or Mg), direct displacement is predicted ($T_{th}=16$ eV and 10 eV, respectively)⁹ and observed at accelerating voltages below 200 kV in the TEM.⁹

Above the threshold energy for the knock-on process, the cross-section for knock-on increases with increasing accelerating voltage. The potential damage due to electron-nuclear interaction becomes more severe as the incoming electron gets more and more energetic. At higher accelerating voltages the electron has enough energy to cause multiple damage events. The quantity, $N_d = \frac{T_{\max}}{2 T_{th}}$, takes into account the possible cascade of damage events. The knock-on damage cross-section includes the cross-section for displacement of an atom directly due to interaction with the electron wave and the probability of being displaced by another "knocked" atom, i.e., $\sigma_{kd} = \sigma_n \times N_d$. Its variation for aluminum in zeolite Y with accelerating voltage is shown in figure 1.



XBL 874-9272 A

Fig. 1. Knock-on and radiolytic damage cross-sections, σ_{kd} and σ_r , respectively, versus accelerating voltage for Al in Y zeolite.

Radiolytic damage

The relativistic cross-section for the interaction between the incident electron and the specimen electron is given by¹⁰

$$\sigma_e = \left(\frac{8 \pi a_0^2 U_R^2}{mc^2} \right) \left(\frac{Z}{T'_{th} \beta^2} \right) \quad (2)$$

where: T'_{th} is the minimum energy that must be transferred to the electrons of the solid to produce atomic nuclear movement (ie., minimum excitation energy for bound or quasi-bound atomic electrons), Z is the number of electrons (usually the atomic number) belonging to the target atom, and a_0 , U_R , mc^2 and β have the meanings described previously. The minimum energy T'_{th} is specific to each different type of atomic site within the specimen and is related to the bond strength and the coordination number of the atom.

The experimental efficiency factor, ζ , for radiolysis in silicates is 0.0001.¹¹ That is, for every ionization event that occurs, the probability of structural rearrangement is 1 in 10,000. The cross-section for radiolytic damage is thus given by

$$\sigma_r = \sigma_e \times \zeta. \quad (3)$$

The behavior of the cross-section for radiolytic damage with accelerating voltage is determined by the parameter β^{-2} . This dependence is illustrated in figure 1 for the case of aluminum in zeolite Y. Note that the cross-section for ionization decreases significantly with increasing accelerating voltage up to 500 kV, then levels off to a constant value.

For zeolites the cross-sections for knock-on and radiolytic damage are of the same order of magnitude (fig. 1), and should both be considered when studying zeolites in the TEM, especially when accelerating voltages above 200 kV are used. Above the knock-on threshold for Al, the damage rate for a zeolite will increase with accelerating voltage rather than decrease, due to the increasing number of direct displacement events.

For aluminosilicates the cross-sections for knock-on and radiolytic damage predict that for an accelerating voltage below 200 kV, the damage should be due to a radiolytic process. The radiolytic cross-section can not, however, predict the actual structural relaxation (i.e., the mechanism) responsible for the damage.

EXPERIMENTAL

Samples of Y zeolite (with sodium cations) with Si/Al-ratios = 2.4, 18 and ∞ were investigated. Specimens for the TEM were prepared by embedding the zeolite powder in LR White acrylic resin and thin sectioning (50-80 nm) with a diamond knife on a Dupont-Sorvall MT-6000 microtome.¹² Sections were floated on water, thus hydrating all specimens equally. The hydrophobic nature of the high Si zeolite is irrelevant when floated on water.

Experiments were carried out in a JEOL 200CX HREM operating between 80 and 200 kV. Typically HREM micrographs are recorded with a current density of $\approx 10^{23} \frac{e}{s} m^{-2}$ ($1.6 \times 10^4 Am^{-2}$), however, to slow the degradation for these experiments lower current densities were used. For specimens with Si/Al-ratios = 2.4 and 18, the current density to the specimen was $1.57 \times 10^{22} \frac{e}{s} m^{-2}$ ($2.51 \times 10^3 Am^{-2}$). For specimens with Si/Al-ratios = ∞ , the current density was $6.28 \times 10^{22} \frac{e}{s} m^{-2}$ ($1.00 \times 10^4 Am^{-2}$); damage at lower current density was too slow to observe within reasonable times. At the higher dose rate the damage rate was observed to decrease slightly with the increased dose rate; but this was within the uncertainty of the measurements. Incident beam current was measured at the image plane with an electrometer and the current density at the specimen was determined using $\phi_{\text{specimen}} = (\text{Mag})^2 \phi_{\text{image}}$ (ϕ = current density). This dependence was verified by measuring the current density at the image plane while maintaining a constant current density at the specimen. Over the magnification range 19,000 to 100,000, the current density measured at the image plane varied inversely with the square of the magnification.

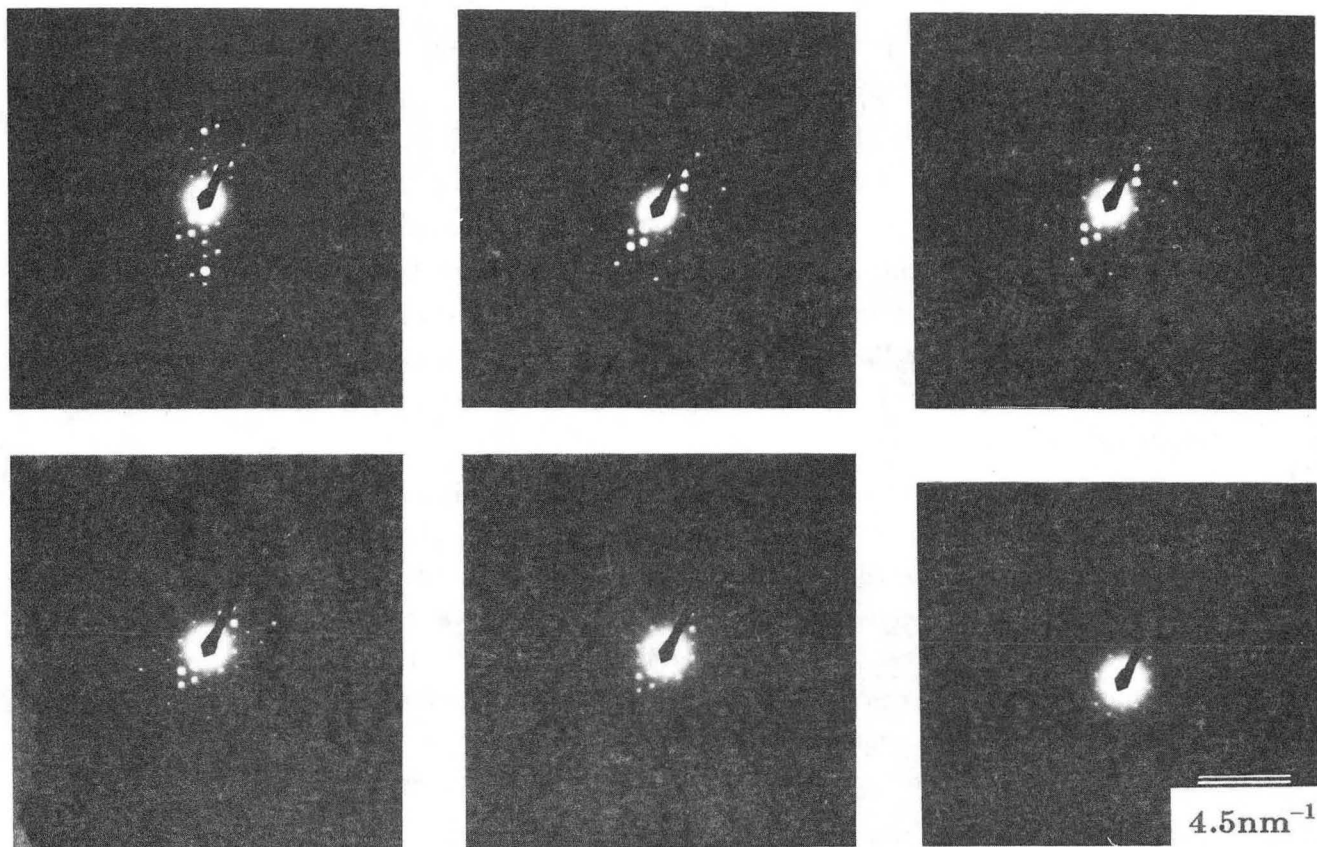
The crystalline to amorphous transformation was monitored by the loss of intensity in the Bragg reflections in the selected area diffraction (SAD) pattern with time. This intensity loss was recorded on photographic film. The end point was determined by invisibility of Bragg reflections on the phosphor image screen in the microscope. This criterion was used in preference to densitometer measurements of the negatives because it is more meaningful to the practicing microscopist. When diffraction spots are no longer visible on the image screen the researcher will assume that the zeolite is amorphous even if the more sensitive photographic film detects some residual crystallinity.

The SAD pattern was taken from a $5 \mu m^2$ region in the center of a $20 \mu m^2$ area of uniform current density. It is the long range periodicity of the crystalline solid that gives rise to strong intensity in the diffraction spots and as this long range periodicity is destroyed the intensity in the spots is reduced. Figure 2 shows some representative diffraction data. The upper three micrographs show the loss of crystallinity in the initial 9 minutes under the electron beam. The lower three micrographs show the final stages of the transformation that took 21 minutes to complete. For each specimen at every accelerating voltage, the transformation was monitored 4 to 5 times to insure the reproducibility of the data. The dose to vitrification was calculated by multiplying the current density by the total time of exposure, until diffraction spots were no longer visible on the TEM screen.

It was assumed that areas adjacent to the $5 \mu m$ diameter probe were not exposed to the electron beam. After one crystal had been transformed, the sample was translated at least $20 \mu m$ to a fresh area and the timer was started for the new crystal.

Si/Al \approx 18

200kV



21m

$$\phi = 1.57 \times 10^{22} \frac{e}{s} m^{-2}$$

XBB 850-8304

Fig. 2. Fading of diffraction spots for specimen with Si/Al=18, at 200 kV, current density = $1.57 \times 10^{22} \frac{e}{s} m^{-2}$ ($2.51 \times 10^3 A m^{-2}$), at times: 5sec, 200sec, 540sec, 780sec, 1080sec, and 1260sec, respectively.

The measurement of current density was accurate to within $\pm 2\%$ for all trials. For specimens with Si/Al-ratios = 2.4 and 18, the transformation time determinations were reproducible with an uncertainty of $\approx \pm 9\%$. This results in an uncertainty in the dose to vitrification of $\approx \pm 9.3\%$. For specimens with Si/Al-ratio = ∞ , transformation time measurements were reproducible with an uncertainty of $\approx \pm 12\%$. The higher uncertainty is probably due to the inhomogeneity of crystal defects in the sample from the dealumination procedures as well as the higher electron current density used. The resulting uncertainty in the dose to vitrification was $\approx \pm 12.2\%$, for specimens with Si/Al-ratio = ∞ .

RESULTS

The metamict transformation took from 5 to 25 minutes to complete, depending on the Si/Al-ratio and the accelerating voltage. The transformation was determined to be independent of orientation, within the uncertainty of the measurements. The dose to vitrification is plotted as a function of accelerating voltage for the three samples in figure 3. For all samples, increasing the accelerating voltage improved their radiation tolerance. This indicates that the damage is radiolytic and that knock-on damage is not significant up to 200 kV accelerating voltage. At 200 kV the difference between the dose to vitrification for the samples with Si/Al-ratios 2.4 and 18 is about 25%; for the sample with Si/Al = ∞ , the dose to vitrification is 3.5 and 5 times greater than that for the samples with Si/Al-ratios 18 and 2.4, respectively. Total replacement of all the aluminum by silicon produces a zeolite that is significantly more stable to electron irradiation as well as to elevated temperatures.

DISCUSSION

Radiolytic degradation of SiO_2 in the TEM has been explained as the weakening of Si-O bonds by the incorporation of H_2O in the structure.¹⁰ Since zeolites are aluminosilicates where the aluminum occupies some of the tetrahedral positions of the silicon, the local structure is the same as SiO_2 , i.e., the Si (or Al) are tetrahedrally coordinated to four O and the radiolytic degradation mechanism could be the same. If this mechanism is responsible for degradation of zeolites then the increase in dose to vitrification with Si/Al-ratio should be explained by the different cross-sections for radiolytic damage for Si and Al in the zeolite structure. Using equation 2, the ratio of the radiolytic cross-sections for an all Si containing zeolite versus an all Al containing zeolite is

$$\frac{\sigma_{\text{Si}}}{\sigma_{\text{Al}}} = 0.80.$$

This predicts that a zeolite structure containing only aluminum atoms (all silicon atoms replaced with aluminum atoms) should degrade with a dose to vitrification 80% that for

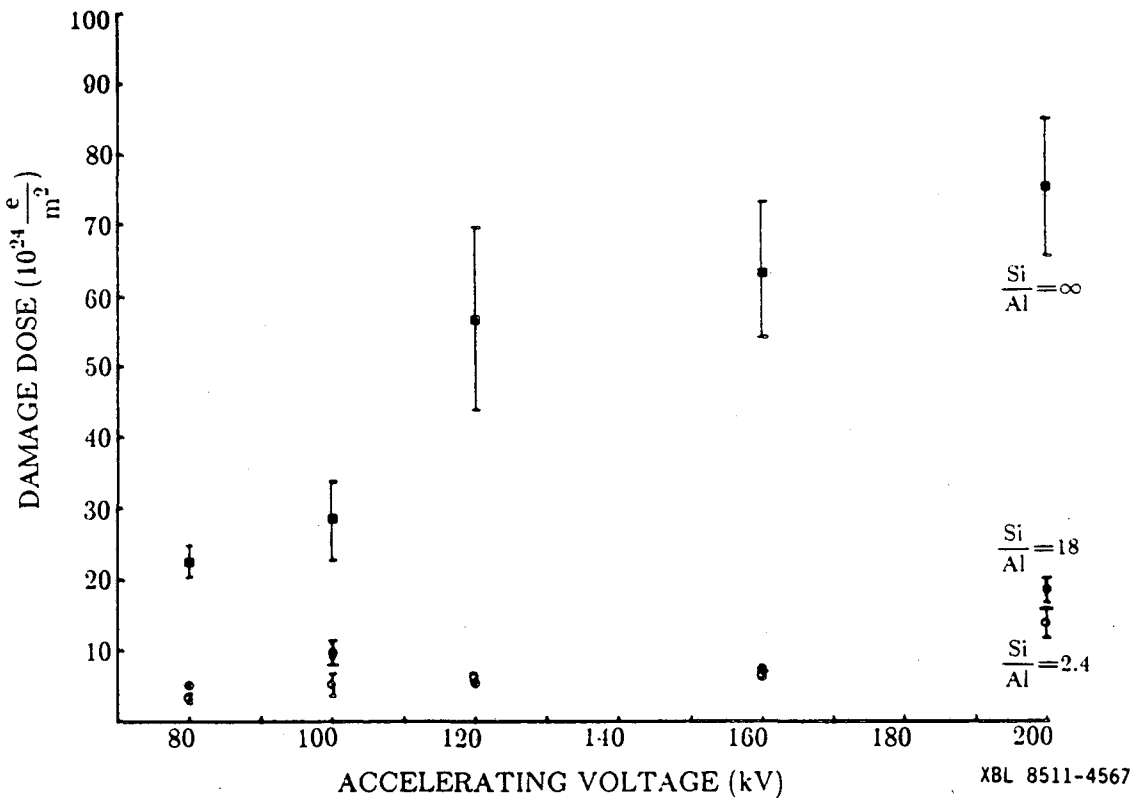


Fig. 3. Dose to vitrification versus accelerating voltage for Y zeolites with Si/Al = 2.4, 18 at current density = $1.57 \times 10^{22} \frac{e}{s} m^{-2}$ ($2.51 \times 10^3 Am^{-2}$), and with Si/Al = ∞ at $6.28 \times 10^{22} \frac{e}{s} m^{-2}$ ($1.00 \times 10^4 Am^{-2}$).

degradation of the same zeolite containing only silicon atoms (all aluminum atoms replaced with silicon atoms). This does not explain the data shown in figure 3, where the sample containing 29% Al (Si/Al=2.4) has a dose to vitrification 20% that of the Si/Al= ∞ sample.

The data in figure 3 indicate that the mechanism and therefore the efficiency of radiolytic damage in zeolites is different from that in quartz. The major differences between the quartz structure and zeolite structures are the openness of the zeolite framework with respect to the quartz structure and the fact that the zeolite may contain measurable amounts of aluminum as a major structural component as well as silicon. The important difference with aluminum in the structure is that each Al has a cation associated with it to balance the framework charge. This cation provides a different mechanism for the degradation of aluminum-containing zeolites. Additionally the openness of the zeolite framework with respect to the quartz structure will contribute to its overall instability.

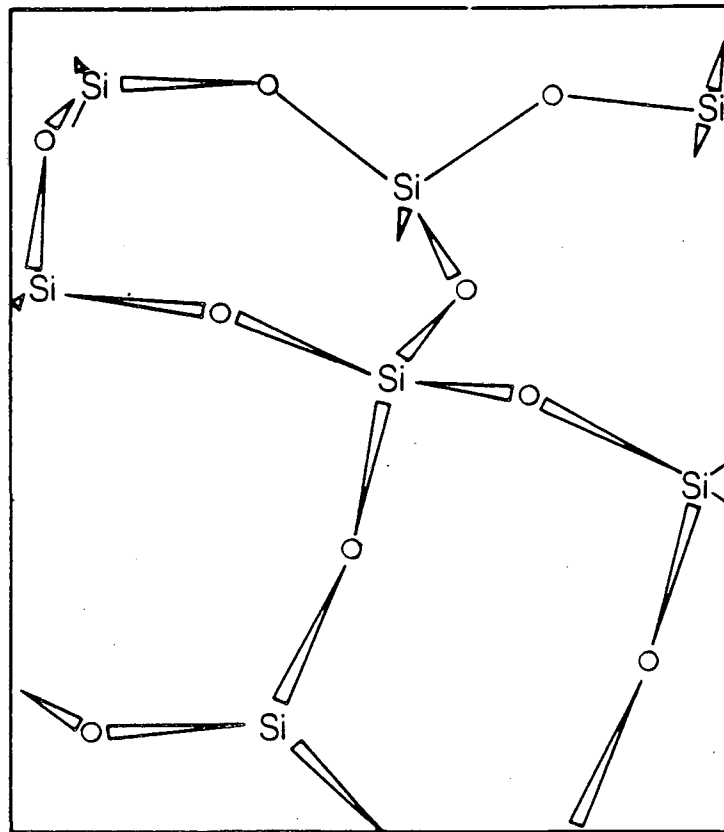
Figure 4 shows a model of a silicon atom tetrahedrally coordinated to four oxygen atoms in the zeolite structure. It is difficult to describe the damage mechanism for a silicon site in a zeolite. If only one Si-O bond is broken the Si atom is rigidly held in place by the three other existing Si-O bonds and the requirement that Si be tetrahedrally coordinated causes the broken Si-O bond to reform without any structural changes. When two Si-O bonds are broken, the Si atom is free to rotate about the two existing Si-O bonds and form bonds in a configuration different from the original structure, however, this leaves some bonds unsatisfied unless several other nearby tetrahedra rotate and reform bonds simultaneously.

Figure 5a shows the case of Al tetrahedrally coordinated to four oxygen atoms in the zeolite framework. If one Al-O bond is broken (fig. 5b), the Al can remain coordinated to only three oxygens and the cation can bond to the fourth oxygen. The Al is stable with three bonds and the cation is still near it for local charge neutrality, but now the structure is permanently changed.

This mechanism can be used to explain why zeolite structures are less electron beam sensitive when dehydrated in vacuo,¹ when sodium ions are exchanged by larger cations,² or when the Si/Al-ratio is increased. The larger the charge compensating cation, the slower its movement into the proper position to bond to the dangling oxygen due to steric hindrance, and the greater the probability for reforming the original Al-O bond and preserving the structure. Therefore at a given Si/Al-ratio, the zeolite with the larger cations will be more stable than the same zeolite framework with smaller cations. The same trend should be observed if the number of cations in the structure is reduced by using cations with greater ionic charge; i.e., Ca^{2+} instead of K^+ . A cation such as La^{3+} should be strongly stabilizing due to its large size and charge. Adsorbed water in the zeolite structure can fill the role of a cation in the damage mechanism. Adsorbed water can bond to the dangling oxygen atom resulting in a structural change at either a Si or an Al site. Thus, dehydrating the zeolite will always enhance its stability under the electron beam regardless of the Si/Al-ratio or type of cation present. As the Si/Al-ratio increases the number of possible degradation sites decreases and the zeolite is more stable to electron irradiation.

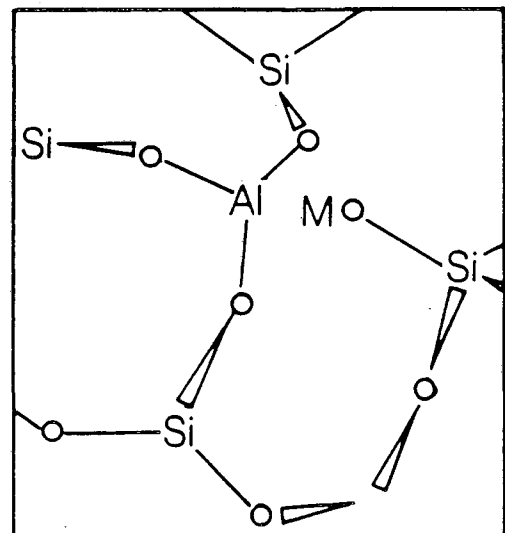
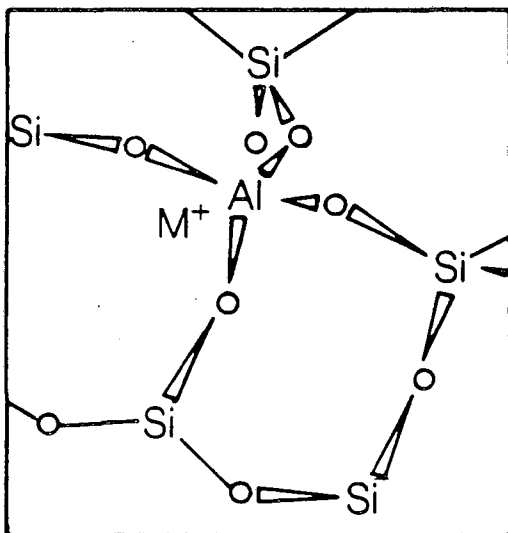
CONCLUSIONS

Experiments have confirmed that the damage of Y zeolites in the TEM is radiolytic and that knock-on damage is not significant in the range 80-200 kV. Experimental evidence suggests a model for the degradation of zeolites in which structural relaxation is enhanced at Al sites due to the presence of a cation. When an Al-O bond is broken, the cation moves into a position to bond to the dangling oxygen atom and the aluminum atom remains bound to only three oxygen atoms. Local charge neutrality is preserved, however, the structure is permanently changed.



-- XBL 874-1948

Fig. 4. Silicon atom tetrahedrally coordinated to four oxygen atoms in the zeolite structure.



-- XBL 874-1949 -

Fig. 5a. Aluminum atom tetrahedrally coordinated to four oxygen atoms in the zeolite structure.
 5b. Aluminum atom coordinated to three oxygen atoms in the damaged zeolite structure.

ACKNOWLEDGEMENTS

We would like to thank Chevron Research Company for providing the various samples of zeolite Y. For many helpful discussions we would like to thank Dr. Ignatius Chan of Chevron Research Company, Dr. Heinz Heinemann of Lawrence Berkeley Laboratory and Dr. Hans-Rudolf Wenk of the University of California at Berkeley.

Specimens were prepared using the facilities at the Electron Microscopy Laboratory, 1581 Life Sciences Building, University of California at Berkeley. This work has been funded by the Director, Office of Energy Research, Office of Basic Energy Sciences, Materials Science Division of the U. S. Department of Energy under Contract No. DE-AC03-76SF00098.

REFERENCES

- 1 Bursill, L. A., Lodge, E. A., and Thomas, J. M., *Nature* (1980) **286** 111
- 2 Bursill, L. A., Thomas, J. M., and Rao, K. J., *Nature* (1981) **289** 157
- 3 Das, G., and Mitchell, T. E., *Rad. Effects* (1974) **23** 49
- 4 Hobbs, L. W., and Pascucci, M. R., *J. Physique* (1980) **41**(C6) 237
- 5 Pabst, A., *Amer. Mineralogist* (1952) **37** 137
- 6 Pascucci, M. R., Hutchinson, J. L., and Hobbs, L. W., *Rad. Effects* (1983) **74** 219
- 7 McKinley, W. A. and Feshbach, H., *Phys. Rev.* (1948) **74** 1759
- 8 Seitz, F., and Koehler, J. S., *Solid State Physics* (1956) **2** 305
- 9 Makin, M. J., *Ninth Int. Cong. On Elect. Micros.* (1978) **III** 330
- 10 Hobbs, L. W., 'Introduction to Analytical Electron Microscopy,' eds. J. J. Hren, J. I. Goldstein and D. C. Joy, Plenum Press, New York, 1979, 437
- 11 Hobbs, L. W., *EMSA Bulletin* (1985) **15** 51
- 12 Csencsits, R., Schooley, C., and Gronsky, R., *J. Elect. Micros. Tech.* (1985) **2** 643

LAWRENCE ~~BERKELEY~~ LABORATORY
TECHNICAL INFORMATION DEPARTMENT
UNIVERSITY OF CALIFORNIA
BERKELEY, CALIFORNIA 94720